



## PERFORMANCE EVALUATION OF DIFFERENT DEEP LEARNING MODELS FOR CLASSIFYING ISCHEMIC, HEMORRHAGIC, AND NORMAL COMPUTED TOMOGRAPHY IMAGES: TRANSFER LEARNING APPROACHES

<sup>1</sup>Mustafa ALTINTAŞ<sup>id</sup>, <sup>2,\*</sup>Muhammet Üsame ÖZİÇ<sup>id</sup>

<sup>1</sup>Konya City Hospital, Department of Neurology, Konya, TÜRKİYE

<sup>2</sup>Pamukkale University, Faculty of Technology, Department of Biomedical Engineering, Denizli, TÜRKİYE

<sup>1</sup>[altintas20@gmail.com](mailto:altintas20@gmail.com), <sup>2</sup>[muozic@pau.edu.tr](mailto:muozic@pau.edu.tr)

### Highlights

- Classification results with different deep-learning models of ischemic stroke, hemorrhagic stroke, and normal computed tomography images are presented.
- Pre-trained deep learning networks have been adjusted for fine-tuning and transfer learning.
- The results have been compared with performance evaluation metrics.
- The result of the study gave promising results in the classification of stroke types and normal images in computed tomography images.



## PERFORMANCE EVALUATION OF DIFFERENT DEEP LEARNING MODELS FOR CLASSIFYING ISCHEMIC, HEMORRHAGIC, AND NORMAL COMPUTED TOMOGRAPHY IMAGES: TRANSFER LEARNING APPROACHES

<sup>1</sup>Mustafa ALTINTAŞ<sup>id</sup>, <sup>2,\*</sup>Muhammet Üsâme ÖZİÇ<sup>id</sup>

<sup>1</sup>Konya City Hospital, Department of Neurology, Konya, TÜRKİYE

<sup>2</sup>Pamukkale University, Faculty of Technology, Department of Biomedical Engineering, Denizli, TÜRKİYE

<sup>1</sup>altintas20@gmail.com, <sup>2</sup>muozic@pau.edu.tr

(Received: 19.08.2023; Accepted in Revised Form: 01.04.2024)

**ABSTRACT:** A stroke is a case of damage to a brain area due to a sudden decrease or complete cessation of blood flow to the brain. The interruption or reduction of the transportation of oxygen and nutrients through the bloodstream causes damage to brain tissues. Thus, motor or sensory impairments occur in the body part controlled by the affected area of the brain. There are primarily two main types of strokes: ischemic and hemorrhagic. When a patient is suspected of having a stroke, a computed tomography scan is performed to identify any tissue damage and facilitate prompt intervention quickly. Early intervention can prevent the patient from being permanently disabled throughout their lifetime. This study classified ischemic, hemorrhage, and normal computed tomography images taken from international databases as open source with AlexNet, ResNet50, GoogleNet, InceptionV3, ShuffleNet, and SqueezeNet deep learning models using transfer learning approach. The data were divided into 80% training and 20% testing, and evaluation metrics were calculated by five-fold cross-validation. The best performance results for the three-class output were obtained with AlexNet as 0.9086±0.02 precision, 0.9097±0.02 sensitivity, 0.9091±0.02 F1 score, 0.9089±0.02 accuracy. The average area under curve values was obtained with AlexNet 0.9920±0.005 for ischemia, 0.9828±0.008 for hemorrhage, and 0.9686±0.012 for normal.

**Keywords:** Computed Tomography, Deep Learning, Hemorrhagic Stroke, Ischemic Stroke, Transfer Learning

### 1. INTRODUCTION

Stroke, the most common cause of disability in the world, is also the third leading cause of death. Stroke, a disease that affects the brain vessels, accounts for more than half of the neurological disorders that require hospitalization. The majority of strokes are of ischemic origin (85%-87%), while the remainder are hemorrhagic strokes (15%-13%). It has been reported that more than 795,000 people have a stroke each year in the United States. In Turkey, cerebrovascular diseases include ischemic strokes with a rate of 72% and hemorrhagic strokes with a rate of 28%. When this disease occurs in different parts of the brain, it causes paralysis in different body parts, which increases the loss of labor and the cost of care. Rapid intervention at the time of stroke is critical in reducing the level of disability as well as prolonging the patient's life expectancy. Therefore, when the disease is diagnosed and the stroke site is quickly identified, the patient's quality of life will improve significantly. Computed tomography (CT) and magnetic resonance (MR) imaging methods are of great importance for the clinical diagnosis of stroke. In the diagnosis of stroke, CT and MR images are interpreted by a specialist radiologist. Because CT images can be obtained more quickly than MR images, they are primarily preferred for early diagnosis. Depending on the test results, the hemorrhage protocol is applied if the bleeding is caused. If the cause is ischemia, the thrombolytic protocol is activated. However, in cases of ischemic stroke, it is important to intervene within the first 3 hours after the onset of symptoms. The new findings show that this time could be extended to 4.5 hours. The rapid diagnosis process helps to save brain tissues with minimal damage with early intervention [1-3].

Medical image analyses are performed by specialist radiologists in hospitals. In radiological image

\*Corresponding Author: Muhammet Üsâme ÖZİÇ, [muozic@pau.edu.tr](mailto:muozic@pau.edu.tr)

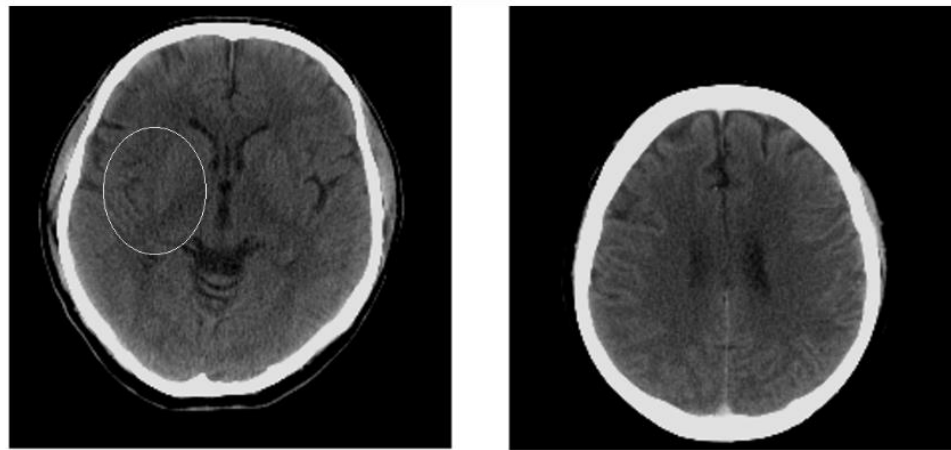
analysis, difficulties such as the necessity of intervention in a short time, problems in accessing specialists who need to interpret images, limitations of facilities in hospitals in small regions, and shortages in the number of radiologists can be encountered. Considering all the disadvantages mentioned, to overcome these shortcomings, the number of studies on image processing and artificial intelligence-based radiological image analysis has been increasing recently and continues to be a hot topic in the literature [4, 5]. Deep learning models have recently been used frequently in the literature for the classification, segmentation, and object detection of medical images [5-7]. In medical studies, where classical machine-learning methods were used for a period, deep-learning models began to be used over time. In classical machine learning methods, features are extracted and classification is performed on the image with different methods. However, there are many different feature extraction methods for this process. Since not every feature is important for classification, then the appropriate feature selection method should be used. Many feature selections can be used for this process as well. There are many feature extraction, feature selection, and machine learning algorithms in this process for the classification application of medical images. Hence, numerous trials are required to determine the most suitable methodology to be applied. In deep learning models, the features on medical images are selected by extracting them along the layers. Therefore, less costly and higher accuracy results can be obtained compared to classical machine learning methods [8]. In the future, it is anticipated that analyzing images on high-speed computers, by pre-processing them and offering doctors preliminary information about the diseases in the images, will become a standard technology in the field of medicine [9]. It may not be predicted whether the cause of stroke is ischemia or hemorrhage in the patient who comes to the emergency room. Because of this, deep learning-based clinical decision support systems can be used as auxiliary tools for the identification of stroke types. In the literature, some studies classify stroke using deep learning algorithms on CT images. However, many of these studies are focused on classifying either ischemic or hemorrhagic strokes [9-28]. Fewer studies simultaneously classify normal, ischemic, and hemorrhagic stroke images [9, 12, 14, 23]. In this study, ischemia, hemorrhage, and normal CT images taken from two different databases were classified using deep learning models. 300 ischemic brain CT images, 300 hemorrhagic brain CT images, and 300 normal brain CT images were used from the databases of the Ischemic Stroke Lesion Segmentation Competition 2018 (ISLES 2018) [29] and the North American Society of Radiology (RSNA) [30]. Data augmentation was applied by performing certain pre-processing steps on the images. The images were randomly divided into 80% training and 20% test data, and validation was performed with 5-fold cross-validation. AlexNet [31], ResNet50 [32], GoogleNet [33], InceptionV3 [34], ShuffleNet [35], and SqueezeNet [36] deep learning models were trained with the transfer learning strategy. The successful performances of the networks were compared with the criteria of precision, recall (sensitivity), F1 score, accuracy, receiver operating characteristic (ROC) curve, the area under the ROC curve (AUC), and training time. As a result of the study, the disease classification performances of the models were compared.

## 2. MATERIAL AND METHODS

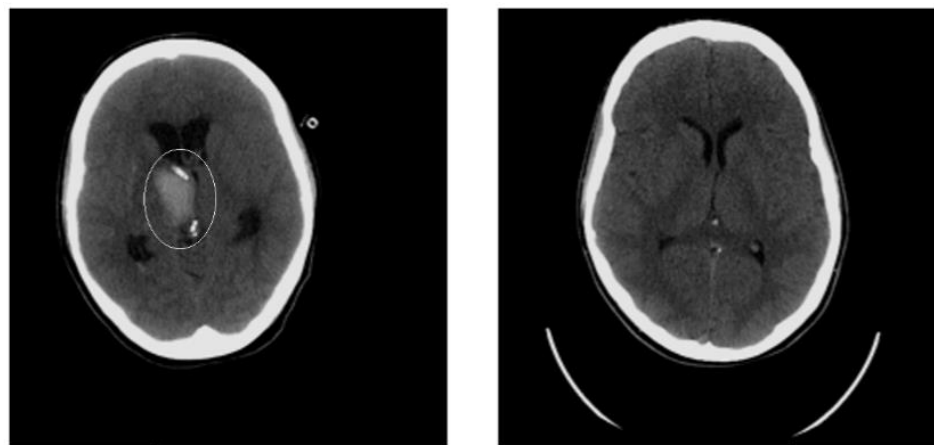
### 2.1. Dataset

In this study, 300 ischemia and 18 normal CT images obtained from the ISLES 2018 (Ischemic Stroke Lesion Segmentation) database [29, 37], 300 hemorrhage and 282 normal CT images obtained from the open source RSNA Intracranial Hemorrhage Detection database published by the Radiological Society of North America were used [30]. The data in DICOM (Digital Imaging and Communications in Medicine) and NIfTI (The Neuroimaging Informatics Technology Initiative) formats were saved as a PNG (Portable Network Graphics) image with a contrast value of 120 and a brightness value of 60 using the MRIcro program [38]. Hemorrhage and ischemia CT slices were determined according to the label information in the databases. Data other than these two labels were filed as normal CT slices. Thus, 300 normal, 300 hemorrhage and 300 ischemia images were collected using multi-center data. Each class was created in equal numbers to avoid an unbalanced data set. Figure 1a shows the ischemic stroke CT slice from the

ISLES dataset, and Figure 1b shows the normal CT slice from the ISLES dataset. Figure 2a shows the hemorrhagic CT slice from the RSNA dataset, and Figure 2b shows the normal CT slice from the RSNA dataset.



(a) (b)  
**Figure 1.** ISLES dataset (a) Ischemic stroke CT slice (b) Normal CT slice [29, 39]



(b) (b)  
**Figure 2.** RSNA dataset (a) Hemorrhagic stroke CT slice (b) Normal CT slice [30, 39]

## 2.2. Deep Learning Models and Transfer Learning

In this study, CT images were classified and the performance of the AlexNet [31], ResNet-50 [32], GoogleNet [33], InceptionV3 [34], ShuffleNet [35], SqueezeNet [36] deep learning models were investigated. All experiments were conducted using the Matlab R2021a program running on a 64-bit Windows operating system with an Intel Core i7-7700HQ CPU 2.80 GHz, 16 GB RAM, and an NVIDIA GeForce GTX 1050 Ti graphics card with 8 GB of memory. The deep learning models in the MATLAB program are already trained with the IMAGENET dataset and produce 1000-class outputs. By using these pre-trained networks, classification can be performed without the need for new training. However, when training with a new dataset, some parameters in the network need to be changed. Thus, pre-trained networks can be used as a starting point for learning a new task. This process, called transfer learning, allows training with the new data set by using pre-trained model weights. In this process, instead of training the network with random weights from scratch by fine-tuning, it becomes quick and easy to perform the training process using the existing pre-trained weights. Fine-tuning a network with transfer learning is often much quicker and more straightforward compared to training a network with

randomly initialized weights from scratch [40]. Transfer learning and fine-tuning processes were carried out by changing the last layers of the six deep learning models used in this study to give three classes of output. These models train according to standard input image size and three-channel color images. CT image sizes should be normalized to 227-by-227 for AlexNet, ShuffleNet, and SqueezeNet, 224-by-224 for GoogleNet and ResNet-50, and 229-by-229 for InceptionV3. CT images were automatically normalized to these dimensions by MATLAB during the training process. Necessary parameter settings were arranged so that the images entered the model inputs as a three-channel color image. In this process, the images were added one after the other, and they acted as if they were colored images. The image contents did not change, they were only converted to the format accepted by the models. Data augmentation was carried out using projection methods and random rotation in the x-direction and y-direction up to 30 pixels. The necessary hyperparameters for measuring the performance results of the models under the same conditions were set as given in Table 1.

**Table 1.** Hyper-parameters for deep learning models [39]

Hyper-parameters	Values
Momentum	0.9
InitialLearnRate	1.00E-04
LearnRateDropFactor	0.2
LearnRateDropPeriod	5
L2Regularization	1.00E-04
GradientThresholdMethod	l2norm
MaxEpochs	7
MiniBatchSize	20
Shuffle	every-epoch
ExecutionEnvironment	GPU
BatchNormalizationStatistics	population

### 2.3. Performance Evaluation Metrics

The training process was performed under equal hyper-parameters for each model and the performance evaluation metrics were calculated. The data used were randomly divided into five parts 80% training and 20% test, one part in each fold was used as test data, and the other four were used as training data. Thus, the images in all data were used in the training and testing process, and the average of the performance values obtained as a result of five-fold cross-validation was calculated. Table 2 shows the five-fold cross-validation strategy for splitting data.

**Table 2.** Five-fold cross-validation strategy

	Data-1 (20%)	Data-2 (20%)	Data-3 (20%)	Data-4 (20%)	Data-5 (20%)
1. Fold	Test	Train	Train	Train	Train
2. Fold	Train	Test	Train	Train	Train
3. Fold	Train	Train	Test	Train	Train
4. Fold	Train	Train	Train	Test	Train
5. Fold	Train	Train	Train	Train	Test

True Positive (TP), True Negative (TN), False Positive (FP), and False Negative (FN) values were determined by creating a confusion matrix for each fold. The values determined as actual and predicted were placed in the confusion matrix as shown in Figure 3 according to the abbreviations expressed below. (I: Ischemic, H: Hemorrhagic, N: Normal )

$CT_{II}$  : Number of correctly classified ischemic images

$CT_{HH}$  : Number of correctly classified hemorrhagic images  
 $CT_{NN}$  : Number of correctly classified normal brain images  
 $CT_{IH}$  : Number of images misclassified as hemorrhagic while ischemic image  
 $CT_{IN}$  : Number of images misclassified as normal brain, while ischemic image  
 $CT_{HI}$  : Number of images misclassified as ischemic while images of hemorrhagic  
 $CT_{HN}$  : Number of images misclassified as normal brain, while hemorrhagic image  
 $CT_{NI}$  : Number of images misclassified as ischemic, while normal image  
 $CT_{NH}$  : Number of images misclassified as hemorrhagic, while normal brain image

		Predicted		
		Ischemic	Hemorrhagic	Normal
Actual	Ischemic	$CT_{II}$	$CT_{IH}$	$CT_{IN}$
	Hemorrhagic	$CT_{HI}$	$CT_{HH}$	$CT_{HN}$
	Normal	$CT_{NI}$	$CT_{NH}$	$CT_{NN}$

**Figure 3.** Confusion Matrix

Performance metrics calculated using TP, TN, FP, and FN values are given in precision Equation 1, recall Equation 2, accuracy Equation 3, and F1-score Equation 4. Cumulative results were obtained for each model by taking the average and standard deviation of the performance values calculated separately for the five folds. Another performance criterion used in this study was the AUC value, which indicates the ROC. ROC curve is one of the graphs used in performance reviews. An AUC value of 1 indicates that the performance is 100% and the classification has been performed fully. The graph is drawn with the false positive rate value corresponding to the true positive rate value of each class. ROC is a probability curve and AUC shows the extent of decomposition. Figure 4 shows the confusion matrix and ROC graph obtained after the first fold of the AlexNet model. These graphs and matrices were created after each fold. Therefore, a total of 30 confusion matrices and 30 ROC graphs were obtained for six deep-learning models. In Figure 5, the flow diagram of the application carried out in this study is given.

$$Precision = \frac{TP}{TP + FP} \tag{1}$$

$$Recall = \frac{TP}{TP + FN} \tag{2}$$

$$F1 - score = 2 * \frac{Precision * Recall}{Precision + Recall} \tag{3}$$

$$Accuracy = \frac{TP + TN}{TP + FN + TN + FP} \tag{4}$$

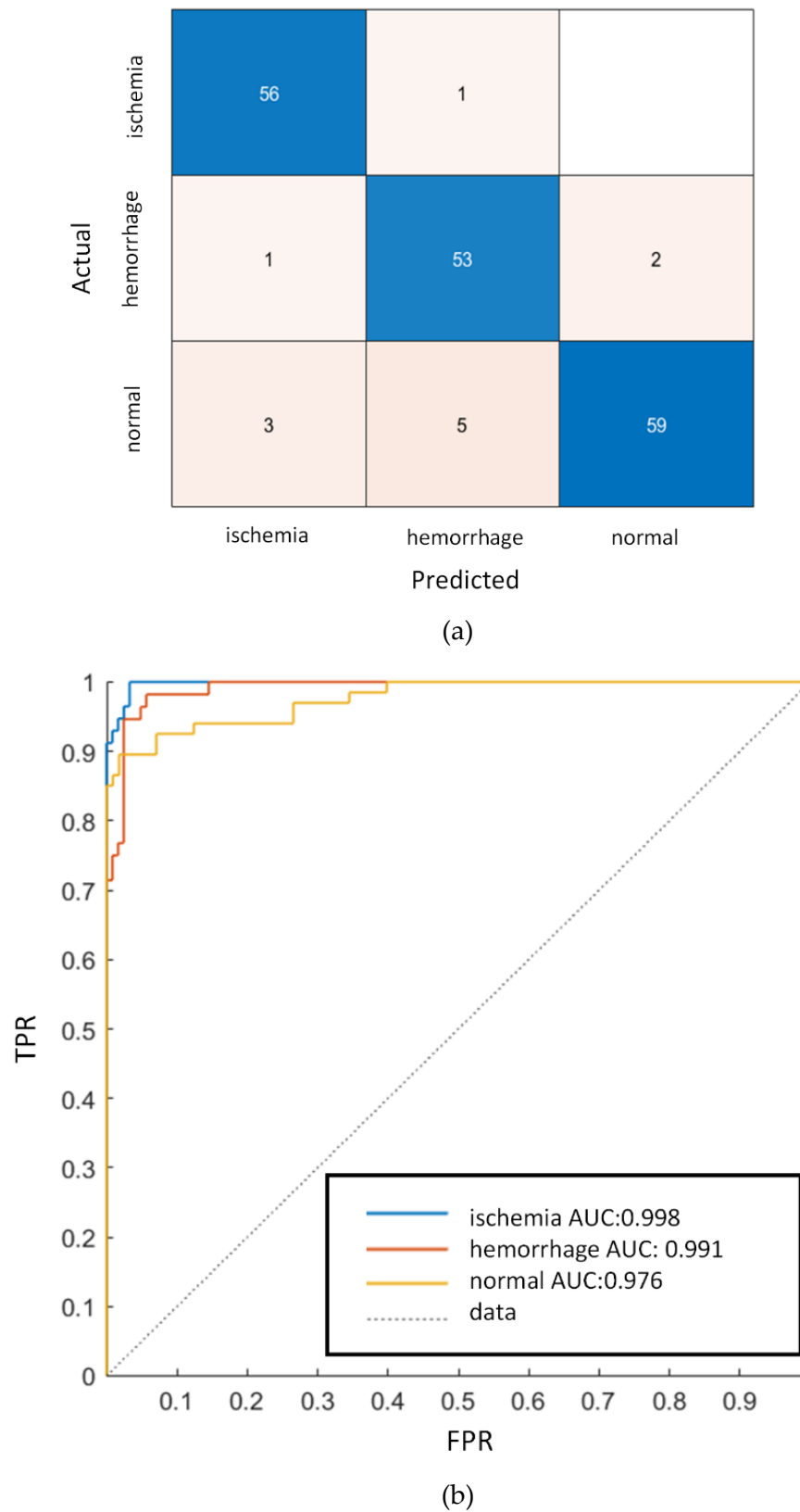


**Figure 4.** (a) Confusion matrix for first fold AlexNet (b) ROC graph for first fold AlexNet [39]

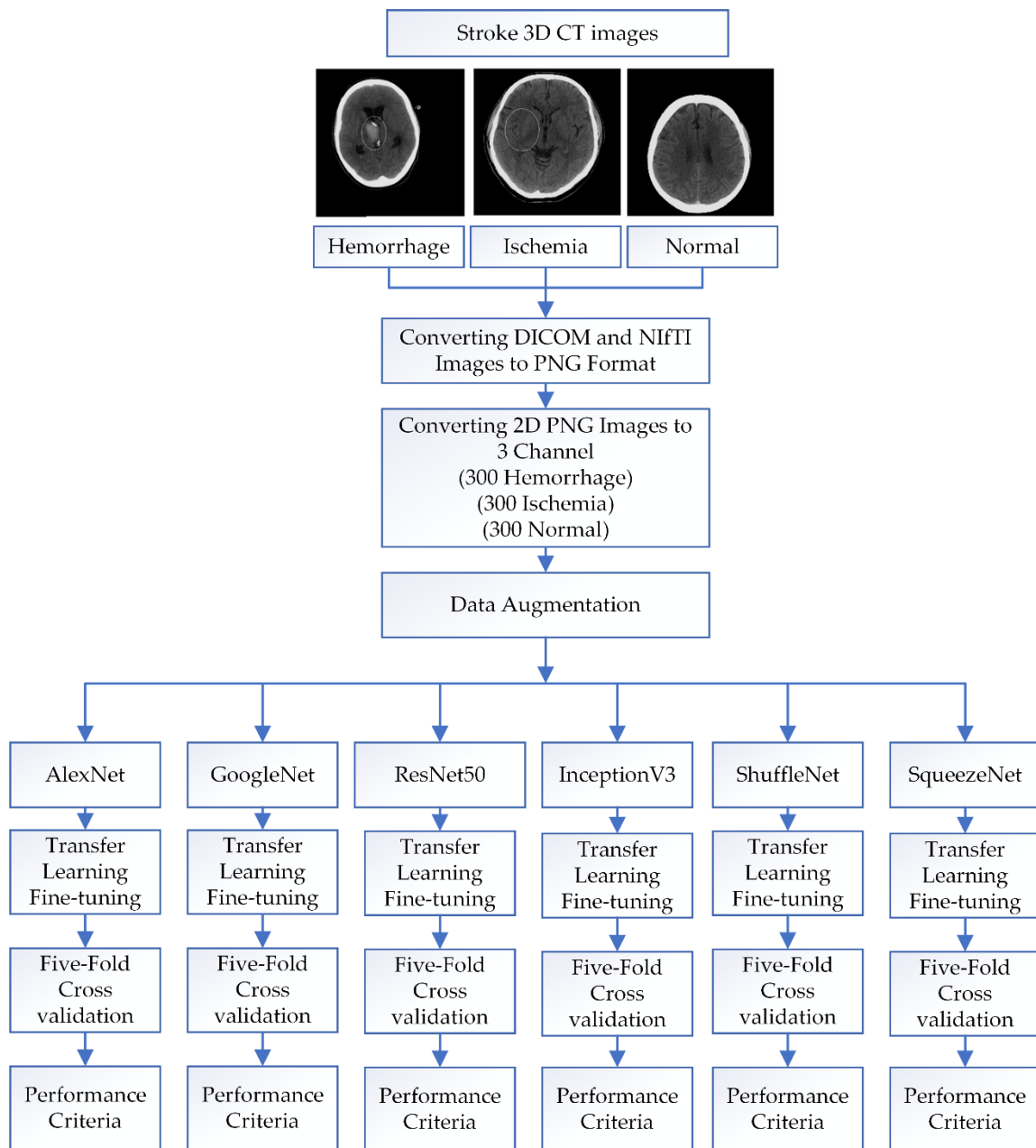


Figure 5. Flow chart of the application performed in this study.

### 3. RESULTS AND DISCUSSION

The average and standard deviation values of the performance criteria obtained as a result of the classification of ischemia, hemorrhage, and normal CT images using six deep learning (DL) models and five-fold cross-validation are given in Table 3.1. At the same time, the average training period is given in the table. In Table 3.2, the average AUC values of all deep learning models obtained according to classes are given.

**Table 3.1.** Performance criteria obtained as a result of the classification of six DL models [39]

DL Models	Precision	Recall	F1-Score	Accuracy	Training Time (hh:mm:ss)
AlexNet	0.9086±0.02	0.9097±0.02	0.9091±0.02	0.9089±0.02	00:21:37
ResNet50	0.9092±0.01	0.9081±0.01	0.9086±0.01	0.9067±0.01	02:33:23
GoogleNet	0.9058±0.019	0.9001±0.024	0.9029±0.021	0.9033±0.019	00:36:10
InceptionV3	0.8772±0.026	0.8781±0.021	0.8777±0.023	0.8778±0.026	00:56:38
ShuffleNet	0.9017±0.014	0.8982±0.018	0.9000±0.016	0.9000±0.015	00:36:27
SqueezeNet	0.8493±0.041	0.8374±0.052	0.8433±0.046	0.8411±0.044	00:16:44

**Table 3.2.** The average AUC values of all DL models [39]

DL Models	Ischemia	Hemorrhage	Normal
AlexNet	0.9920±0.005	0.9828±0.008	0.9686±0.012
ResNet50	0.9918±0.003	0.9856±0.003	0.9688±0.009
GoogleNet	0.9900±0.005	0.9794±0.004	0.9628±0.011
InceptionV3	0.9872±0.007	0.971±0.012	0.9432±0.025
ShuffleNet	0.9882±0.006	0.9784±0.003	0.9558±0.017
SqueezeNet	0.9874±0.005	0.9488±0.020	0.9358±0.027

When examining Table 3.1, the lowest average training time was 00:21:37 (hh:mm:ss), and the highest average accuracy result was 0.9089±0.02 from the AlexNet deep learning model. Although the classification performance values were generally close to each other, AlexNet yielded slightly higher results with fewer layers and a shorter training time. Although SqueezeNet had the shortest training time, it achieved the lowest result with an accuracy value of 0.8411±0.044. In general, it was observed that successful results were obtained in the classification of CT images using the transfer learning method of deep learning models. The average values of the area under the curve were calculated as 0.9920±0.005 for ischemia, 0.9828±0.008 for hemorrhage, and 0.9686±0.012 for normal using AlexNet. There are studies in the literature for the detection and classification of stroke with deep learning models and CT images [9-28]. However, many studies classify either hemorrhage or ischemia. In some studies, CT segmentation applications of the stroke-related region are carried out with different deep-learning models [13, 17, 41-44]. There are also studies that use MR images, which are acquired over a longer duration compared to CT images, to perform stroke classification [45-52]. The number of studies classifying normal, ischemia, and hemorrhage CT images is limited [9, 12, 14, 23]. Although studies have shown successful results in detecting only ischemia or hemorrhage, a person who arrives at the hospital with a suspected stroke cannot have only hemorrhage or ischemia. A patient who arrives with a suspected stroke can have one of three possibilities on the CT image: normal, ischemia, or hemorrhage. Therefore, deep learning-based clinical decision support systems capable of predicting and detecting these three classes can generate quick results for diagnosis. The applications and experiments conducted in this study have been carried out with this motivation. Dourado et al. developed an IoT system using deep learning for feature extraction and classical machine learning algorithms for classification. They used CT images of 140 normal cases, 140 hemorrhagic cases, and 140 ischemic cases. The dataset consisted of DICOM and grayscale images from two different databases, but no information about the data collection centers was provided. The data was split into 80% for training and 20% for testing, and classification experiments were performed using 10-fold cross-validation. For DICOM images, combining all convolutional neural network (CNN) architectures with various machine learning classifiers resulted in 100% accuracy, F1-score, recall, and precision. The highest accuracy rates were obtained when the classifiers were combined with InceptionV3, MobileNet, and VGG16 architectures. Similarly, for grayscale images, combining CNN architectures with different classifiers resulted in 100%

accuracy, F1-score, recall, and precision. The experiments showed that the highest accuracies were observed when different classifiers were combined with the NASNet Large architecture. The study used a transfer learning approach but did not mention data augmentation and the AUC metric [9]. Gautam and Raman created two different data sets in their study (Himalayan Institute of Medical Sciences (HIMS) in Dehradun, India). The first dataset consists of 192 brain images of two different classes: hemorrhagic stroke and ischemic stroke. The second data set is a data set containing three categories of brain CT scans (hemorrhagic stroke, ischemic stroke, and normal). This data set consists of a total of 900 brain images and includes 300 images for each category. Pre-processing techniques and image fusion were applied to enhance image quality. In this study, the approaches of transfer learning and data augmentation were not mentioned. Performance metrics including precision, TPR, FPR, F-measure, and accuracy were calculated. For the experiments to be performed on the first data set, the data set was divided into 70% training and 30% testing, and for the experiments on the second data set, the data set was divided into 80% training and 20% testing. Additionally, 10-fold cross-validation was applied in both experiments. In the first data set, the highest accuracy rate was obtained by the proposed CNN model called P\_CNN with 98.33%. In the second data set, the highest accuracy rate was again obtained by the P\_CNN model with 92.22%. [14]. Neethi et al. collected 3D CT images of 70 ischemic, 68 hemorrhagic, and 96 normal cases from the Sree Chitra Tirunal Institute for Medical Sciences and Technology (Trivandrum, India). A three-output classification study was carried out by developing a 3D CNN model with 3D CT images. The data was divided into 60% for training, 20% for validation, and 20% for testing to perform the model's performance. Data augmentation, cross-validation, and transfer learning approach were not used. The model performance result was 0.88 F1-score, 0.84 recall, 0.94 precision, and 0.92 accuracy. ROC and AUC values were not calculated. A voxel-based evaluation was made because it was a study using a 3D CNN model [23]. Pereira et al., with support from Clinical Trajano Almeida, collected a total of 100 normal, 100 ischemic, and 100 hemorrhagic CT images. Using the Particle Swarm Optimization method, a CNN model was optimized and utilized for classification. As a result of the study, a classification rate close to 99% was achieved. However, the study did not mention the utilization of transfer learning, cross-validation, or the AUC approach [12]. As observed in the studies, different deep learning models, images from various centers, varying data quantities, distinct performance criteria, diverse transfer learning, and data augmentation strategies, all contribute to significantly complexify result comparisons. Generally, high accuracy rates have been reported for three-class outputs. The differences in data quantities introduce uncertainties regarding how the diagnosis would perform across the entire stroke population. In this study, promising outcomes were achieved on data obtained from distinct centers and protocols. Especially the AUC values being very close to 100% indicate the substantial separability of one group from the others.

#### 4. CONCLUSIONS

In this study, ischemia, hemorrhage, and normal CT images were classified using the transfer learning method in six different deep-learning models. The AlexNet model gave higher classification results than other models. Rapid diagnosis of hemorrhage and ischemia in CT images of patients suspected of having a stroke is essential. However, several factors can complicate stroke diagnosis, including time constraints, lack of experience, variations in interpretation based on experience, approximate pixel tone distributions in the images, confusion between hemorrhage and ischemia, a large number of images requiring evaluation in hospitals, and challenges in accessing doctors or radiologists in smaller cities. Because of this, deep learning-based clinical decision support systems can provide the opportunity for rapid diagnosis and early treatment. In advanced applications, the size, localization, and three-dimensional models of strokes can be developed using deep learning segmentation models. By developing mobile and desktop applications and embedding deep learning models that perform predictive tasks in the background, assistant diagnostic tools for doctors can be expected as a future technology in the field of medicine. In this study, it is clear that clinical decision support systems based on deep learning show significant potential in distinguishing and categorizing stroke types. However,

further research is needed in this area, which requires the use of comprehensive datasets covering various stroke subtypes, as well as the inclusion of standard assessment methodologies.

### Acknowledgments

This study was carried out by Mustafa ALTINTAŞ as a master's thesis in the Department of Biomedical Engineering at Necmettin Erbakan University, Graduate School of Natural and Applied Sciences.

### Declaration of Ethical Standards

The authors declare that there are no ethical standards.

### Credit Authorship Contribution Statement

MA contributed to data processing, creation and running of models, calculation of performance evaluation metrics, and article writing. MÜÖ contributed to article writing and literature review.

### Declaration of Competing Interest

There is no conflict of interest.

### Funding / Acknowledgements

There is no funding.

### Data Availability

The authors used ISLES 2018 and RSNA datasets. These datasets are available to researchers and free of charge.

### REFERENCES

- [1] M. Şahan, S. Satar, A. F. Koç, and A. Sebe, "İskemik İnme ve Akut Faz Reaktanları," *Arşiv Kaynak Tarama Dergisi*, vol. 19, no. 2, pp. 85-140, 2010.
- [2] M. Emre, "Nöroloji Temel Kitabı," Ankara: Güneş Tıp Kitapevleri, ch. 669-792, p. 1616, 2013.
- [3] C. W. Tsao *et al.*, "Heart disease and stroke statistics—2023 update: a report from the American Heart Association," *Circulation*, vol. 147, no. 8, pp. e93-e621, 2023.
- [4] R. Karthik, R. Menaka, A. Johnson, and S. Anand, "Neuroimaging and deep learning for brain stroke detection-A review of recent advancements and future prospects," *Computer Methods and Programs in Biomedicine*, p. 105728, 2020.
- [5] F. Yuce, M. Ü. Öziç, and M. Tassoker, "Detection of pulpal calcifications on bite-wing radiographs using deep learning," *Clinical Oral Investigations*, vol. 27, no. 6, pp. 2679-2689, 2023.
- [6] H. P. Chan, L. M. Hadjiiski, and R. K. Samala, "Computer-aided diagnosis in the era of deep learning," *Medical Physics*, vol. 47, no. 5, pp. e218-e227, 2020.
- [7] H. Fujita and technology, "AI-based computer-aided diagnosis (AI-CAD): the latest review to read first," *Radiological Physics*, vol. 13, no. 1, pp. 6-19, 2020.
- [8] C. Park, C. C. Took, and J.-K. Seong, "Machine learning in biomedical engineering," *Biomedical Engineering Letters*, vol. 8, pp. 1-3, 2018.
- [9] C. M. Dourado Jr, S. P. P. da Silva, R. V. M. da Nobrega, A. C. d. S. Barros, P. P. Reboucas Filho, and V. H. C. J. C. N. de Albuquerque, "Deep learning IoT system for online stroke detection in skull computed tomography images," *Computer Networks*, vol. 152, pp. 25-39, 2019.

- [10] T. D. Phong *et al.*, "Brain hemorrhage diagnosis by using deep learning," in *Proceedings of the 2017 International Conference on Machine Learning and Soft Computing*, 2017, pp. 34-39.
- [11] C.-L. Chin *et al.*, "An automated early ischemic stroke detection system using CNN deep learning algorithm," in *2017 IEEE 8th International Conference on Awareness Science and Technology (iCAST)*, Taiwan, 2017: IEEE, pp. 368-372.
- [12] D. R. Pereira, P. P. Reboucas Filho, G. H. de Rosa, J. P. Papa, and V. H. C. de Albuquerque, "Stroke lesion detection using convolutional neural networks," in *2018 International Joint Conference on Neural Networks (IJCNN)*, 2018: IEEE, pp. 1-6.
- [13] A. Majumdar, L. Brattain, B. Telfer, C. Farris, and J. Scalera, "Detecting intracranial hemorrhage with deep learning," in *2018 40th Annual International Conference of the IEEE Engineering in Medicine and Biology Society (EMBC)*, 2018: IEEE, pp. 583-587.
- [14] A. Gautam and B. Raman, "Towards effective classification of brain hemorrhagic and ischemic stroke using CNN," *Biomedical Signal Processing Control*, vol. 63, p. 102178, 2021.
- [15] J. Pan, G. Wu, J. Yu, D. Geng, J. Zhang, and Y. Wang, "Detecting the Early Infarct Core on Non-Contrast CT Images with a Deep Learning Residual Network," *Journal of Stroke Cerebrovascular Diseases*, vol. 30, no. 6, p. 105752, 2021.
- [16] C.-M. Lo, P.-H. Hung, and D.-T. Lin, "Rapid Assessment of Acute Ischemic Stroke by Computed Tomography Using Deep Convolutional Neural Networks," *Journal of Digital Imaging*, pp. 1-10, 2021.
- [17] Y. Watanabe *et al.*, "Improvement of the diagnostic accuracy for intracranial haemorrhage using deep learning-based computer-assisted detection," *Neuroradiology*, vol. 63, no. 5, pp. 713-720, 2021.
- [18] K. L. Gia *et al.*, "A Computer-Aided Detection to Intracranial Hemorrhage by Using Deep Learning: A Case Study," presented at the Green Technology and Sustainable Development 2020, Da Nang Eyaleti, Vietnam, 2020.
- [19] A. M. Dawud, K. Yurtkan, and H. Oztoprak, "Application of deep learning in neuroradiology: Brain haemorrhage classification using transfer learning," *Computational Intelligence Neuroscience*, vol. 2019, 2019.
- [20] S.-M. Jung and T.-K. Whangbo, "A Deep Learning System for Diagnosing Ischemic Stroke by Applying Adaptive Transfer Learning," *Journal of Internet Technology*, vol. 21, no. 7, pp. 1957-1968, 2020.
- [21] O. Öman, T. Mäkelä, E. Salli, S. Savolainen, and M. Kangasniemi, "3D convolutional neural networks applied to CT angiography in the detection of acute ischemic stroke," *European Radiology Experimental*, vol. 3, no. 1, pp. 1-11, 2019.
- [22] Y. Shinohara, N. Takahashi, Y. Lee, T. Ohmura, and T. Kinoshita, "Development of a deep learning model to identify hyperdense MCA sign in patients with acute ischemic stroke," *Japanese Journal of Radiology*, vol. 38, no. 2, pp. 112-117, 2020.
- [23] A. Neethi, S. Niyas, S. K. Kannath, J. Mathew, A. M. Anzar, and J. Rajan, "Stroke classification from computed tomography scans using 3d convolutional neural network," *Biomedical Signal Processing and Control*, vol. 76, p. 103720, 2022.
- [24] O. Ozaltin, O. Coskun, O. Yeniay, and A. Subasi, "A Deep Learning Approach for Detecting Stroke from Brain CT Images Using OzNet," *Bioengineering*, vol. 9, no. 12, p. 783, 2022.
- [25] S. Korra, R. Mamidi, N. R. Soora, K. V. Kumar, and N. C. S. Kumar, "Intracranial hemorrhage subtype classification using learned fully connected separable convolutional network," *Concurrency and Computation: Practice and Experience*, vol. 34, no. 24, p. e7218, 2022.
- [26] A. A. M. Suberi, W. N. W. Zakaria, R. Tomari, A. Nazari, M. N. H. Mohd, and N. F. N. Fuad, "Deep transfer learning application for automated ischemic classification in posterior fossa CT images," *International Journal of Advanced Computer Science and Applications*, vol. 10, no. 8, 2019.
- [27] B. A. Mohammed *et al.*, "Multi-method diagnosis of CT images for rapid detection of intracranial hemorrhages based on deep and hybrid learning," *Electronics*, vol. 11, no. 15, p. 2460, 2022.

- [28] T. H. Gençtürk, F. K. Gülağiz, and K. İsmail, "Derin Öğrenme Yöntemleri Kullanılarak BT Taramalarında Beyin Kanaması Teşhisinin Karşılaştırmalı Bir Analizi," *Journal of Intelligent Systems: Theory and Applications*, vol. 6, no. 1, pp. 75-84, 2023.
- [29] A. Hakim *et al.* "Ischemic Stroke Lesion Segmentation." Available: <http://www.isleschallenge.org/> [Accessed: May 7, 2020].
- [30] RSNA. "Intracranial Hemorrhage Detection." Radiological Society of North America. Available: <https://www.kaggle.com/c/rsna-intracranial-hemorrhage-detection/rules> [Accessed: Oct. 30, 2020].
- [31] A. Krizhevsky, I. Sutskever, and G. E. Hinton, "Imagenet classification with deep convolutional neural networks," *Advances in neural information processing systems*, vol. 25, pp. 1097-1105, 2012.
- [32] K. He, X. Zhang, S. Ren, and J. Sun, "Deep residual learning for image recognition," in *Proceedings of the IEEE Conference on Computer Vision and Pattern Recognition*, 2016, pp. 770-778.
- [33] C. Szegedy *et al.*, "Going deeper with convolutions," in *Proceedings of the IEEE Conference on Computer Vision and Pattern Recognition*, 2015, pp. 1-9.
- [34] C. Szegedy, V. Vanhoucke, S. Ioffe, J. Shlens, and Z. Wojna, "Rethinking the inception architecture for computer vision," in *Proceedings of the IEEE Conference on Computer Vision and Pattern Recognition*, 2016, pp. 2818-2826.
- [35] X. Zhang, X. Zhou, M. Lin, and J. Sun, "Shufflenet: An extremely efficient convolutional neural network for mobile devices," in *Proceedings of the IEEE Conference on Computer Vision and Pattern Recognition*, 2018, pp. 6848-6856.
- [36] F. N. Iandola, S. Han, M. W. Moskewicz, K. Ashraf, W. J. Dally, and K. Keutzer, "SqueezeNet: AlexNet-level accuracy with 50x fewer parameters and < 0.5 MB model size," *arXiv preprint arXiv:1602.07360*, 2016.
- [37] C. W. Cereda *et al.*, "A benchmarking tool to evaluate computer tomography perfusion infarct core predictions against a DWI standard," *Journal of Cerebral Blood Flow & Metabolism*, vol. 36, no. 10, pp. 1780-1789, 2016.
- [38] Neuroimaging Informatics Tools and Resources Clearinghouse. "MRIcro." McCausland Brain Imaging Center. Available: <https://www.nitrc.org/projects/mricro/> [Accessed: Oct. 20, 2020].
- [39] M. Altıntaş, "Classification of Stroke with Different Deep Learning Models in Computerized Tomography Images," Master's Thesis, Department of Biomedical Engineering, Graduate School of Natural and Applied Sciences, Necmettin Erbakan University, Türkiye, 2021.
- [40] Z. N. K. Swati *et al.*, "Brain tumor classification for MR images using transfer learning and fine-tuning," *Computerized Medical Imaging and Graphics*, vol. 75, pp. 34-46, 2019.
- [41] M. Soltanpour, R. Greiner, P. Boulanger, and B. Buck, "Ischemic Stroke Lesion Prediction in CT Perfusion Scans Using Multiple Parallel U-Nets Following by a Pixel-Level Classifier," in *2019 IEEE 19th International Conference on Bioinformatics and Bioengineering (BIBE)*, 2019: IEEE, pp. 957-963.
- [42] S. Yalçın and H. Vural, "Brain stroke classification and segmentation using encoder-decoder based deep convolutional neural networks," *Computers in Biology and Medicine*, vol. 149, p. 105941, 2022.
- [43] I. Guerrón, N. Pérez, D. Benítez, F. Grijalva, D. Riofrío, and M. Baldeon-Calisto, "Extending the U-Net Architecture for Strokes Segmentation on CT Scan Images," in *2023 IEEE 13th International Conference on Pattern Recognition Systems (ICPRS)*, 2023: IEEE, pp. 1-7.
- [44] S. Yalcin, "Hybrid Convolutional Neural Network Method for Robust Brain Stroke Diagnosis and Segmentation," *Balkan Journal of Electrical and Computer Engineering*, vol. 10, no. 4, pp. 410-418, 2022.
- [45] Z. Liu, C. Cao, S. Ding, Z. Liu, T. Han, and S. J. I. A. Liu, "Towards clinical diagnosis: Automated stroke lesion segmentation on multi-spectral MR image using convolutional neural network," *IEEE Access*, vol. 6, pp. 57006-57016, 2018.

- [46] L. Chen, P. Bentley, and D. Rueckert, "Fully automatic acute ischemic lesion segmentation in DWI using convolutional neural networks," *NeuroImage: Clinical*, vol. 15, pp. 633-643, 2017.
- [47] A. Clèrigues *et al.*, "Acute and sub-acute stroke lesion segmentation from multimodal MRI," *Computer Methods and Programs in Biomedicine*, vol. 194, p. 105521, 2020.
- [48] J. Hong, H. Cheng, Y.-D. Zhang, and J. Liu, "Detecting cerebral microbleeds with transfer learning," *Machine Vision Applications*, vol. 30, no. 7, pp. 1123-1133, 2019.
- [49] Y. Yu *et al.*, "Use of deep learning to predict final ischemic stroke lesions from initial magnetic resonance imaging," *JAMA Network Open*, vol. 3, no. 3, pp. e200772-e200772, 2020.
- [50] L. Zhang *et al.*, "Ischemic Stroke Lesion Segmentation Using Multi-Plane Information Fusion," *IEEE Access*, vol. 8, pp. 45715-45725, 2020.
- [51] R. Zhang *et al.*, "Automatic segmentation of acute ischemic stroke from DWI using 3-D fully convolutional DenseNets," *IEEE Transactions on Medical Imaging*, vol. 37, no. 9, pp. 2149-2160, 2018.
- [52] C. U. Perez Malla, M. d. C. Valdes Hernandez, M. F. Rachmadi, and T. Komura, "Evaluation of enhanced learning techniques for segmenting ischaemic stroke lesions in brain magnetic resonance perfusion images using a convolutional neural network scheme," *Frontiers in Neuroinformatics*, vol. 13, p. 33, 2019.